

PTO-MAIN
RM 862.7.44

STIC-ILL

From: Davis, Minh-Tam
Sent: Monday, June 30, 2003 3:26 PM
To: STIC-ILL
Subject: Reprint request for 09/061417

- 1) Armstrong, AT, 1998, J Amer College Cardiology 32(3): 704-10
- 2) Stetson, SJ, 2001, Circulation, 104(6): 676-81.
- 3) Schwitter, J, 1999, J heart Lung Transplantation, 18(10): 1003-13.
- 4) Beltrami, CA, 1994, Circulation, 89(1): 151-63.
- 5) Leenen F H; Holliswell D L; Cardella C J

Department of Medicine, Toronto Western Hospital, Canada.
American heart journal (UNITED STATES) Oct 1991, 122 (4 Pt 1)
p1087-94 ISSN 0002-8703 Journal Code: 0370465

- 6) Ho Y L; Chen C L; Hsu R B; Lin L C; Yen R F; Lee C M; Chen M F; Huang P J
Department of Internal Medicine (Cardiology), National Taiwan University
Hospital, No. 7, Chung-Shan S. Road, Taipei, Taiwan.
Ultrasound in medicine & biology (England) Feb 2001, 27 (2) p171-9,
ISSN 0301-5629 Journal Code: 0410553

Thank you.

MINH TAM DAVIS
ART UNIT 1642, ROOM 8A01, MB 8E12
305-2008



● *Original Contribution*

ASSESSMENT OF THE MYOCARDIAL CHANGES IN HEART TRANSPLANT RECIPIENTS WITHOUT EVIDENT ACUTE MYOCARDIAL REJECTION BY INTEGRATED BACKSCATTER: COMPARISON WITH SIMULTANEOUS DOBUTAMINE STRESS ECHOCARDIOGRAPHY AND $^{201}\text{THALLIUM}$ SPECT

YI-LWUN HO,* CHI-LONG CHEN,† RON-BIN HSU,‡ LUNG-CHUN LIN,* RUOH-FANG YEN,§
CHII-MING LEE,* MING-FONG CHEN* and POR-JAU HUANG*

Departments of *Internal Medicine (Cardiology), †Pathology, ‡Surgery and §Nuclear Medicine, National Taiwan University Hospital, Taipei, Taiwan

(Received 5 June 2000; in final form 1 September 2000)

Abstract—Cardiomyocyte hypertrophy and interstitial fibrin deposition develop in cardiac allografts and contribute to the functional changes of transplanted hearts. We hypothesized that integrated backscatter (IBS) can detect these myocardial changes. A total of 32 heart transplant recipients with either no or mild acute rejection (International Society of Heart and Lung Transplantation grade IA) were enrolled in this study. IBS data of myocardium were collected immediately before simultaneous dobutamine stress echocardiography (DSE) and $^{201}\text{thallium}$ imaging. Coronary angiography and endomyocardial biopsy were also performed. Coronary angiography showed diffuse narrowing in 1 patient who also had abnormal results of IBS, DSE, and thallium results. In the other 31 patients with patent coronary arteries, there were 3 patients (10%) with abnormal DSE results, 19 patients (61%) with abnormal IBS patterns, and 16 patients (52%) with reversible thallium perfusion defects. Of the patients, 44% had cardiomyocyte hypertrophy and 56% interstitial fibrin deposition. There were significant differences in the prevalence of $^{201}\text{thallium}$ perfusion defects and serum cyclosporine levels between patients with and without abnormal IBS patterns. Pathologic changes were also associated with abnormal IBS patterns ($p = 0.01$). However, there was no association between abnormal IBS and DSE results. By multiple logistic regression analysis, the abnormal IBS patterns were associated inversely with serum cyclosporine level ($p = 0.028$). In conclusion, abnormal IBS patterns are associated significantly with perfusion heterogeneity and pathologic changes in heart transplant recipients without evident acute myocardial rejection. There is no association between abnormal IBS patterns and dobutamine-induced dyssynergy in these patients. IBS provides a noninvasive approach for detection of myocardial changes in transplanted hearts without evident acute rejection. (E-mail: porjau@ha.mc.ntu.edu.tw) © 2001 World Federation for Ultrasound in Medicine & Biology.

Key Words: Integrated backscatter, Heart transplantation, $^{201}\text{Thallium}$ perfusion scan, Dobutamine stress echocardiography.

INTRODUCTION

Several studies have reported that cardiac allografts undergo some cardiomyocyte hypertrophy after heart transplantation (Armstrong et al. 1998; Pickering and Boughner 1990; Rowan and Billingham 1990). These histologic alterations may contribute to the functional changes of the transplanted hearts, particularly myocardial stiffness, diastolic dysfunction and, to a certain extent, systolic

dysfunction (Armstrong et al. 1998; Schulman et al. 1993; Valentine et al. 1989). On the other hand, interstitial fibrin deposition in biopsies of transplanted hearts has been reported to identify patients at high risk for developing coronary artery disease or graft failure (Labarre et al. 1998). Therefore, noninvasive detection of these myocardial changes has clinical significance. Ultrasonic tissue characterization with integrated backscatter (IBS) mode has been used to detect acute cardiac allograft rejection, myocardial ischemia and viability (Angermann et al. 1997; Castaldo et al. 2000; Lin et al. 1998a, 1998b; Masuyama et al. 1990; Takiuchi et al. 1998; Wickline et al. 1985). The changes in IBS are

Address correspondence to: Por-Jau Huang, M.D., Department of Internal Medicine (Cardiology), National Taiwan University Hospital, No. 7, Chung-Shan S. Road, Taipei, Taiwan. E-mail: porjau@ha.mc.ntu.edu.tw

caused by variations in myocardial collagen or water content, myofibril orientation relative to the incident ultrasound (US) beam (Finch-Johnston et al. 1999, 2000) and myocardial contractile performance (O'Brien et al. 1995; Wickline et al. 1985). Therefore, we hypothesized that IBS could assess cardiomyocyte hypertrophy and interstitial fibrin deposition in heart transplant recipients without evident acute myocardial rejection. The aims of this study were: 1. to evaluate the IBS of heart transplant recipients without or with minimal acute myocardial rejection (International Society of Heart and Lung Transplantation grade 0 or IA); 2. to compare the results of IBS with those of simultaneous dobutamine stress echocardiography (DSE) and $^{201}\text{Thallium}$ perfusion imaging; and 3. to compare the results of IBS with pathology of endomyocardial biopsy.

METHODS

Study population

A total of 32 heart transplant recipients (27 men and 5 women) were enrolled in this study. The mean recipient age was 50 ± 12 years and mean donor age was 32 ± 11 years. The mean posttransplant duration was 31 ± 22 months (12 to 108 months). All patients received triple-drug immunosuppressive therapy according to our heart transplantation protocol (Hsu et al. 1999). Cyclosporine was started po within 5 days after transplantation or after the recovery of renal function. Cyclosporine dosage was adjusted according to renal function and serum cyclosporine level, which was maintained at the trough level of 300 to 500 ng/mL during the first 3 months after transplantation and adjusted 1 year after transplantation with a mean cyclosporine level of 235 ± 120 ng/mL. Azathioprine was given at 1 to 2 mg/kg/day after transplantation, with the dose adjusted to maintain the white blood cell count with a mean of $6349 \pm 1624/\text{mm}^3$. Prednisolone (0.5 mg/kg/day) was started on the second postoperative day and tapered to 0.2 mg/kg/day by the first month after transplantation. Endomyocardial biopsy was performed weekly in the first month, biweekly in the second month, monthly in the sixth month and yearly sixth month after transplantation. Endomyocardial biopsy of these patients showed either no ($n = 20$) or grade IA ($n = 12$) acute rejection at time of entry into this study. Tacrolimus (FK506) was used in 4 patients for recurrent rejection or severe adverse reactions to cyclosporine and azathioprine. Hypertriglyceridemia was treated by bezafibrate. Hypercholesterolemia was treated by pravastatin and acipimox. Hypertension was treated with angiotensin-converting enzyme inhibitors and calcium channel blockers. Echocardiographic left ventricular mass index was calculated according to the method of Devereux and Reichek (1977), and was

considered to be increased if it exceeded $100 \times \text{g}/\text{m}^2$ in women and $130 \times \text{g}/\text{m}^2$ in men (Levy et al. 1987).

All patients underwent examinations of IBS immediately before simultaneous DSE and $^{201}\text{Thallium}$ single-photon emission computed tomography (SPECT). Serum biochemistry, cyclosporine levels, cardiac catheterization and endomyocardial biopsy were performed within 2 weeks after the above examinations. A total of 38 segments with good echocardiographic windows in 15 controls who had normal coronary angiography were used to calculate the normal data of IBS.

IBS data acquisition

The IBS data were collected with a special software package (Acoustic Densitometry) developed by Hewlett-Packard and incorporated into a commercially available echocardiograph (SONOS 2500) as described in our laboratory (Lin et al. 1998a, 1998b). This system is capable of providing images in which grey levels were displayed proportional to the IBS amplitude. The imaging frame rate was automatically set to 30 frames/s and the dynamic range of the IBS signal was approximately 40 dB. A total of 60 frames from consecutive cardiac cycles were displayed after scan conversion and were stored on the optic disk.

The parasternal short-axis view at the papillary muscle level was used to obtain the 2-D image of IBS (Fig. 1). The transmit power and time gain compensation were adjusted to optimize image presentation, and remained constant throughout the study. The IBS was quantified by placing a 21×21 pixel region of interest in the myocardium on the frozen image. The region-of-interest (ROI) was kept frame by frame to fit within the boundary of subendocardial myocardium and to avoid specular endocardial and epicardial echoes throughout the cardiac cycle. The infero-septum and lateral wall were not used for IBS data collection due to the unreliability of IBS parameters (Castaldo et al. 2000; Finch-Johnston et al. 1999, 2000). For each patient, 3 ROIs were chosen in the same short axis image. One was at the midanteroseptal area (region 1 in Fig. 1; left anterior descending artery, LAD, territory), another was at the midinferior area (region 2 in Fig. 1; right coronary artery, RCA, territory), and the other was at the junction of midposterior with midlateral area (region 3 in Fig. 1; left circumflex artery, LCX, territory). The serial time-varying changes in the magnitude of IBS (in dB) were then obtained from each frame during the cardiac cycle and displayed as a curve of IBS vs. time with electrocardiographic R-wave as a reference. The images and data sets were stored in the optic disc for off-line analysis. For most patients, the curve included more than two consecutive beats.

IBS data analysis

We determined the amplitude (in dB) of cyclic variation of IBS as the difference between minimal and maximal

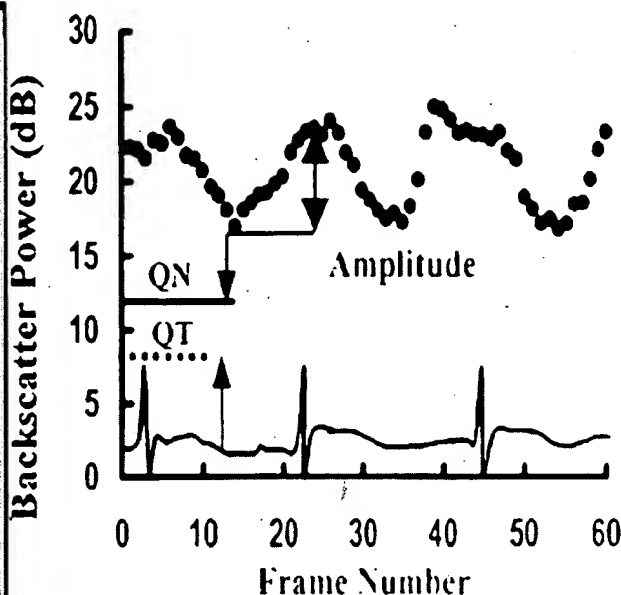
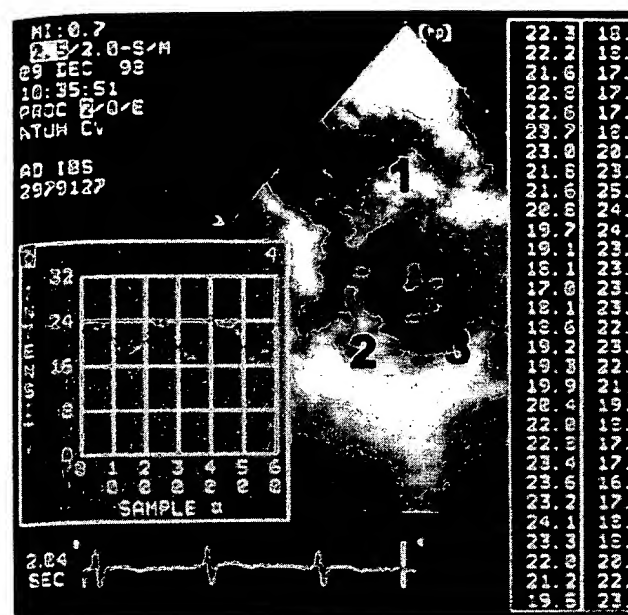


Fig. 1. Left panel shows the acquisition of IBS from the parasternal short axis view. Region 1 represents antero-septal area (LAD territory), region 2 represents the midinferior area (RCA territory), and region 3 represents the junction of midlateral and midposterior area (LCX territory). Right panel shows that the amplitude is defined as the difference between minimal and maximal values in a cardiac cycle; QN interval = the interval from the upstroke of QRS complex to the nadir of the cyclic variation; QT interval = the interval from the upstroke of QRS complex to the end of T wave of electrocardiograph. The vertical axis is the intensity of IBS (decibels) and the horizontal axis is frame number (30 frames/s).

values in a cardiac cycle average at least 2 consecutive beats. After measuring the interval from the upstroke of QRS complex to the nadir of the cyclic variation (QN interval), we divided the value by QT interval to determine the phase (unitless) (Castaldo et al. 2000; Finch-Johnston et al. 1999, 2000; Takiuchi et al. 1998). We also compensated the amplitude of cyclic variation with respect to the phase of regional contraction. In this study, a mean of phase in normal control was 1.0 ± 0.1 . If the ratio > 1.2 or < 0.8 (mean ± 2 SD of normal), we considered it indicative of asynchronous (or delayed) contraction or passive stretching (Lin et al. 1998a, 1998b; Takiuchi et al. 1998). The phase-compensated amplitude was approximated and calculated as follows:

$$\begin{aligned}
 \text{factor} &= -1 && \text{if } (\text{ratio} \leq 0.2); \quad (1) \\
 \text{factor} &= \cos[(\text{ratio} - 0.8) \div 0.6] \times 180^\circ && \text{if } (0.2 < \text{ratio} < 0.8) \\
 \text{factor} &= 1 && \text{if } (0.8 \leq \text{ratio} \leq 1.2) \\
 \text{factor} &= \cos[(\text{ratio} - 1.2) \div 0.6] \times 180^\circ && \text{if } (1.2 < \text{ratio} < 1.8) \\
 \text{factor} &= -1, && \text{if } (1.8 \leq \text{ratio})
 \end{aligned}$$

(Lin et al. 1998a; Wickline et al. 1985, 1986).

The interobserver variation for amplitude and phase were 8% and 7%, respectively (Lin et al. 1998a). The intraobserver variation for amplitude and phase were 5% and 4%, respectively.

DSE protocol

The DSE was performed according to the protocol described previously (Ho et al. 1999). Dobutamine was given IV at rates of 5, 10, 20, 30 and 40 $\mu\text{g}/\text{kg}/\text{min}$ in 3-min stages. Standard parasternal and apical views were obtained. The left ventricle was divided into 16 segments according to guidelines of the American Society of Echocardiography (Schiller et al. 1989). Images were generated with a SONOS 2500 apparatus (Hewlett-Packard, Andover, MA) with a 2.0–2.5-MHz probe, digitized and then stored in quad-screen cine loop format with a Freeland Cardiac Workstation (Louisville, CO) for the online and off-line wall motion analysis. The images taken at baseline, during the 10 $\mu\text{g}/\text{kg}/\text{min}$ infusion and after 5 min recovery were recorded as the resting, low-dose, and recovery images. The images taken at the highest attainable infusion rate were recorded as the peak-dose images. The echocardiographers had no knowledge of IBS, thallium or angiographic results.

Wall motion analysis

Wall motion was analyzed by two experienced echocardiologists who reviewed the digital cine loop images with no knowledge of IBS, thallium or angiographic results. The following scoring system was used: 1 = segments with normal or hyperkinetic motion; 2 = hypokinesia; 3 = akinesia; and 4 = dyskinesia (Schiller et al. 1989). Myocardial ischemia was considered present if new or worsening regional wall motion abnormality was induced by dobutamine. Akinesia directly deteriorated to dyskinesia was not considered to be a marker of myocardial ischemia (Arnese et al. 1994). Our interobserver agreement for DSE was 94% ($\kappa = 0.85$, SEM = 0.078) (Ho et al. 1998).

Dobutamine $^{201}\text{thallium}$ imaging

$^{201}\text{Thallium}$ (2 to 3 mCi) was injected IV at peak phase during dobutamine infusion according to the protocol described previously (Huang et al. 1998). $^{201}\text{Thallium}$ SPECT was carried out within 10 min (stress phase) and at 4 h (redistribution phase) after the injection of $^{201}\text{Thallium}$ using a large field-of view gamma camera (Starcam 3000, General Electric, Milwaukee, WI) equipped with a low-energy, all-purpose collimator. The detector collected data through a 180° arc from the 45° right anterior oblique to the 45° left posterior oblique position. Contiguous transaxial tomograms were reconstructed into 6-mm thick multiple sections, using a filtered back-projection method, with a Hanning ramp filter. Thereafter, the tomographic slices were reorganized to obtain standard short-axis, horizontal long-axis and vertical long-axis views for analysis.

SPECT analysis

All SPECT images were interpreted qualitatively by two experienced observers. We used the 16-color scale in image interpretation. The left ventricle was divided into 10 segments, as proposed by Iskandrian et al. (1987). $^{201}\text{Thallium}$ activity in each segment was graded as 3 (normal), 2 (mildly reduced), 1 (moderately reduced), or 0 (severely reduced or absent). A segment was considered abnormal if its grade was 2 or less (Huang et al. 1998). Stress images were compared with redistribution images to evaluate the presence or absence of reversible or fixed perfusion defects (Fig. 2). Reverse redistribution was considered present when there was a decrease in regional tracer uptake of ≥ 1 grade at redistribution phase as compared to stress images. For correlating coronary artery anatomy, the septum and the anterior segments were considered to belong to the LAD territory, the inferior segments to the RCA territory, and the lateral segment to the LCX territory. The apex did not define any particular vascular distribution. If apex alone was involved, it was allocated to the LAD territory

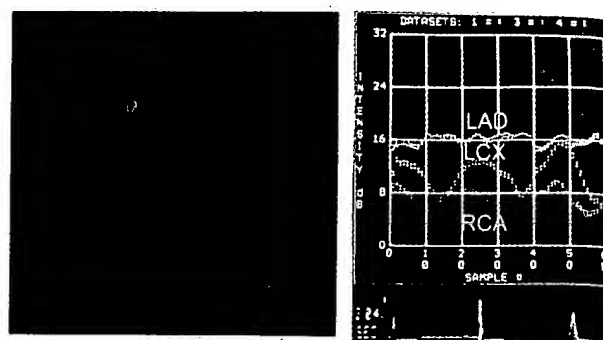


Fig. 2. Left panel shows the $^{201}\text{thallium}$ imaging of a patient at peak phase of dobutamine infusion (upper row) and the same regions at redistribution phase (lower row). There are reversible perfusion defects in the antero-septal, midseptal and midinferior segments. Right panel shows the IBS curve of the same patient. The IBS of the antero-septal area (LAD territory) shows decreased amplitude and loss of cyclic variation. The IBS of junction at midlateral and midposterior area (LCX territory) shows a normal sine-curve. The IBS of the midinferior area (RCA territory) shows delayed contraction (abnormal QN/QT ratio) relative to the curve of LCX.

(Senior et al. 1994). Our interobserver agreement for SPECT interpretation was 96% ($\kappa = 0.90$, SEM = 0.079) (Ho et al. 1995).

Pathologic examination

All 32 patients had biopsy specimens available for evaluation of acute rejection, cardiomyocyte hypertrophy and interstitial fibrin deposition (Labarrere et al. 1998; Rowan and Billingham 1990; Winters and Schoen 1997). The myocyte diameters within the field were measured using standard criteria (Unverferth et al. 1986). All of the longitudinally directed myocytes with a distinct cell border (at the level of the nucleus) were measured and averaged to provide the mean cardiomyocyte diameter (Armstrong et al. 1998). Cardiomyocyte hypertrophy was defined by a myocyte diameter $> 40 \mu\text{m}$ (Schoen 1999).

Cardiac catheterization

Right-side cardiac catheterization, endomyocardial biopsy and coronary angiography were performed using standard procedures. A $\geq 50\%$ diameter stenosis or diffuse narrowing was considered significant. Left ventricular ejection fraction was calculated by area-length method from the left ventriculogram.

Statistical analysis

All data were expressed as mean \pm SD. Statistical differences among the groups were obtained by using the student's *t*-test and chi-square methods. Multiple logistic regression analysis was used to analyze the relation be-

Table 1. Characteristics of patients in group A and group B

	Group A (n = 20)	Group B (n = 12)	p value
Donor age (years)	29 ± 10	37 ± 10	NS
Recipient age (years)	51 ± 14	47 ± 8	NS
Posttransplantation duration (months)	30.6 ± 23.3	31.1 ± 21.4	NS
Ischemic time (min)	115 ± 52	111 ± 48	NS
Rejection numbers	5 ± 3	5 ± 2	NS
²⁰¹ Thallium reversible defects (patients)	14	3	0.035
Hypertension (patients)	5	7	NS
Diabetes mellitus (patients)	4	3	NS
Hyperlipidemia (patients)	7	4	NS
Men/women	18/2	9/3	NS
Body mass index (kg per m ²)	39.0 ± 2.3	39.1 ± 3.6	NS
Blood urea nitrogen (mmol/L)	11.4 ± 3.0	10.8 ± 2.6	NS
Creatinine (μmol/L)	159 ± 35	159 ± 44	NS
Calcium (mmol/L)	2.38 ± 0.13	2.36 ± 0.09	NS
Cyclosporin concentration (ng/mL)	188 ± 74	334 ± 142	0.016
Cholesterol (mmol/L)	5.64 ± 1.19	5.20 ± 1.06	NS
Triglyceride (mmol/L)	1.68 ± 0.77	2.61 ± 1.06	0.008
Uric acid (μmol/L)	512 ± 137	500 ± 107	NS
Glucose (mmol/L)	6.1 ± 1.0	7.4 ± 5.1	NS
Globulin (mg/L)	37 ± 5	39 ± 9	NS
Hemoglobin (gm/L)	125 ± 20	123 ± 20	NS
Hematocrit (fraction of 1.00)	0.37 ± 0.06	0.37 ± 0.05	NS
White blood cell count (/mm ³)	6398 ± 1829	6269 ± 1282	NS
Baseline heart rate (beats/min)	94 ± 11	86 ± 13	NS
Baseline systolic pressure (mmHg)	137 ± 16	133 ± 21	NS
Peak-dose heart rate (beats/min)	151 ± 12	140 ± 19	0.048
Peak-dose systolic pressure (mmHg)	169 ± 31	162 ± 39	NS
Left ventricular ejection fraction (%)	63 ± 10	63 ± 8	NS
Pulmonary capillary wedge pressure (mmHg)	11 ± 5	12 ± 6	NS
Pulmonary artery systolic pressure (mmHg)	28 ± 5	30 ± 9	NS
Pulmonary artery diastolic pressure (mmHg)	11 ± 5	13 ± 6	NS
Right ventricular systolic pressure (mmHg)	30 ± 6	32 ± 8	NS
Right ventricular diastolic pressure (mmHg)	5 ± 4	6 ± 5	NS
Left ventricular diastolic pressure (mmHg)	12 ± 7	12 ± 5	NS

NS = nonsignificant.

tween variables. It was considered statistically significant if $p < 0.05$. Interobserver concordance was determined by calculating the kappa (κ) coefficient.

RESULTS

Patient characteristics

Among the 32 patients, there were 12 with hypertension, 7 with diabetes mellitus, and 11 patients with hyperlipidemia. There were 7 patients with echocardiographic left ventricular hypertrophy. The mean left ventricular ejection fraction was 63 ± 9%. The baseline and peak-dose heart rate were 91 ± 12 and 147 ± 16 beats/min ($p < 0.0001$). The baseline and peak-dose systolic blood pressure were 136 ± 18 and 167 ± 34 mmHg ($p < 0.0001$). Coronary angiography showed diffuse narrowing in 1 patient who also had abnormal DSE, IBS and thallium results. In the other 31 patients with patent coronary arteries, there were 3 patients (10%) with abnormal DSE results, 19 patients (61%) with abnormal IBS patterns and 16 patients (52%) with reversible perfusion defects.

IBS data

The normal values of IBS collected from 38 segments of healthy controls were: amplitude, 7.3 ± 1.5 dB; phase, 1.0 ± 0.1; and phase-compensated amplitude, 7.3 ± 1.5 dB. Of the 96 segments (32 patients) analyzed, 63 segments (group I) showed normal IBS data (all of the amplitude, phase, and phase-compensated amplitudes were in the ranges of mean ± 2 SD of healthy controls). Another 33 segments (group II) had abnormal IBS data (at least one of the amplitude, phase, and phase-compensated amplitudes was outside the above ranges). The prevalence of ²⁰¹thallium reversible perfusion defects was significantly different between groups I and II (21% vs. 52%; $p = 0.004$).

Of the 32 patients studied, 20 (group A) had 1 or more segments with IBS data outside the ranges of mean ± 2 SD of healthy controls, and the other 12 patients (group B) had normal IBS data. Significant variables between these two groups were (Table 1): ²⁰¹thallium reversible perfusion defects (70% vs. 25%, $p = 0.035$), peak-dose heart rates (151 ± 12 vs. 140 ±



Fig. 3. Pathology of endomyocardial biopsy (H & E stain, 20 \times) shows cardiomyocyte hypertrophy and interstitial fibrin deposition with clot formation (arrowheads).

19 beats/min, $p = 0.048$), serum levels of cyclosporine (188 ± 74 vs. 334 ± 142 ng/mL, $p = 0.016$) and triglyceride (1.68 ± 0.77 vs. 2.61 ± 1.06 mmol/L, $p = 0.008$). By multiple logistic regression analysis, the abnormal IBS patterns were associated inversely with serum concentrations of cyclosporine ($p = 0.028$).

DSE results

There were 4 patients with abnormal DSE results. All of them had abnormal $^{201}\text{thallium}$ perfusion defects and abnormal IBS patterns. The agreement between DSE and IBS was 50% ($\kappa = 0.16$). The agreement between DSE and $^{201}\text{thallium}$ SPECT was 59% ($\kappa = 0.22$).

$^{201}\text{thallium}$ SPECT

A total of 30 segments with reversible perfusion defects were noted in 17 patients. There were another 11 patients with reverse redistribution patterns. No patients had fixed perfusion defects. Abnormal segments were localized as follows: septal and anterior wall 37%, inferior wall 40%, and posterior-lateral wall 23%. There were no significant variables in patients with or without perfusion defects, except serum cyclosporine levels. The prevalence of a normal $^{201}\text{thallium}$ pattern was 67% in patients with serum cyclosporine levels ≥ 300 ng/mL and 0% in those with levels < 300 ng/mL ($p < 0.001$). The agreement of IBS with $^{201}\text{thallium}$ SPECT was 72% ($\kappa = 0.43$, $p = 0.007$).

Pathologic findings

A total of 25 patients had abnormal pathologic findings: 14 patients with cardiomyocyte hypertrophy and 18 patients with interstitial fibrin deposition (Fig. 3). The pulmonary wedge pressure, pulmonary artery pressure, right and left ventricular pressures were similar

between patients with and without abnormal pathologic findings (Table 2). There were no other significant clinical variables between patients with or without cardiomyocyte hypertrophy, except white blood cell counts (7025 ± 1753 vs. 5824 ± 1339 mm 3 , $p = 0.036$). There were no significant clinical variables between patients with or without interstitial fibrin deposition, except the recipient age (54 ± 12 vs. 44 ± 11 years, $p = 0.026$).

The prevalence of normal IBS patterns was 24% in patients with abnormal pathologic findings and 86% in those with normal findings (Table 2, $p = 0.01$). The baseline and peak-dose heart rates were significantly higher in patients with abnormal pathologic findings (93 ± 13 vs. 85 ± 4 beats/min, $p = 0.013$; 150 ± 12 vs. 136 ± 23 beats/min, $p = 0.038$). There was no statistical significance between serum cyclosporine level and pathologic changes (312 ± 153 vs. 219 ± 109 ng/mL, $p = 0.116$). The prevalence of normal thallium pattern was 12% in patients with abnormal pathologic findings and 29% in those with normal findings ($p = \text{nonsignificant}$).

DISCUSSION

Heterogeneity of myocardial perfusion in heart transplant recipients

As early as 1 year after heart transplantation, intimal thickening and coronary arteriosclerosis are detectable with histologic examinations and intracoronary ultrasound in up to 75% of patients, despite normal angiographic findings (Johnson et al. 1991; St Goar et al. 1992; Yeung et al. 1995). The cardiac allograft vasculopathy is thought to progress through repetitive endothelial injury followed by repair response (Weis and von Scheidt 1997). DSE is reported to increase the diagnostic sensitivity of vasculopathy documented by intravascular ultrasound (Spes et al. 1999). On the other hand, abnormal results (reverse redistribution, reversible and persistent defects) of $^{201}\text{thallium}$ scintigraphy have also been reported in 40% of transplantation recipients despite normal coronary angiography (Puskas et al. 1997). In the present study, there were 3 (10%) of 31 patients with patent coronary angiography and abnormal DSE results. However, 16 of these 31 patients had reversible perfusion defects. The prevalence of a normal $^{201}\text{thallium}$ pattern was 67% in our patients with serum cyclosporine levels ≥ 300 ng/mL and 0% in those with levels < 300 ng/mL ($p < 0.001$). Sufficient immunosuppression with cyclosporine has been reported to inhibit intimal thickening and intimal cell accumulation of rat cardiac allografts in a dose-dependent fashion (Koskinen et al. 1995). Using a predictive model for adverse cardiac events from cardiac allograft vasculopathy in cohort studies, Mehra and others detected a prognostic impact

Table 2. Characteristics of patients with normal and abnormal pathological findings

	Abnormal (n = 25)	Normal (n = 7)	p value
Donor age (years)	31 ± 11	34 ± 9	NS
Recipient age (years)	50 ± 13	47 ± 8	NS
Posttransplantation duration (months)	28 ± 22	42 ± 22	NS
Ischemic time (min)	111 ± 50	111 ± 40	NS
Rejection numbers	5 ± 3	5 ± 2	NS
²⁰¹ Thallium reversible defects (patients)	14	3	NS
Abnormal IBS patterns (patients)	19	1	0.01
Hypertension (patients)	9	3	NS
Diabetes mellitus (patients)	5	2	NS
Hyperlipidemia (patients)	10	1	NS
Body mass index (kg per m ²)	38.9 ± 2.5	39.4 ± 3.9	NS
Blood urea nitrogen (mmol/L)	11.0 ± 3.0	11.7 ± 2.2	NS
Creatine (μmol/L)	150 ± 35	177 ± 35	NS
Calcium (mmol/L)	2.37 ± 0.12	2.38 ± 0.08	NS
Cyclosporine concentration (ng/ml)	219 ± 109	312 ± 153	NS
Cholesterol (mmol/L)	5.56 ± 1.16	5.22 ± 1.11	NS
Triglyceride (mmol/L)	1.86 ± 0.86	2.63 ± 1.2	NS
Uric acid (μmol/L)	494 ± 131	553 ± 77	NS
Glucose (mmol/L)	6.2 ± 1.9	8.0 ± 6.7	NS
Globulin (mg/L)	37 ± 5	40 ± 11	NS
Hemoglobin (g/L)	122 ± 21	132 ± 13	NS
Hematocrit (fraction of 1.00)	0.37 ± 0.06	0.38 ± 0.04	NS
White blood cell count (/mm ³)	6306 ± 1745	6503 ± 1190	NS
Baseline heart rate (beats/min)	93 ± 13	85 ± 4	0.013
Baseline systolic pressure (mmHg)	137 ± 16	131 ± 24	NS
Peak-dose heart rate (beats/min)	150 ± 12	136 ± 23	0.038
Peak-dose systolic pressure (mmHg)	166 ± 32	169 ± 42	NS
Left ventricular ejection fraction (%)	63 ± 9	64 ± 10	NS
Pulmonary capillary wedge pressure (mmHg)	11 ± 5	11 ± 5	NS
Pulmonary artery systolic pressure (mgHg)	29 ± 7	29 ± 4	NS
Pulmonary artery diastolic pressure (mmHg)	12 ± 6	11 ± 5	NS
Right ventricular systolic pressure (mmHg)	30 ± 7	32 ± 4	NS
Right ventricular diastolic pressure (mmHg)	6 ± 4	7 ± 5	NS
Left ventricular diastolic pressure (mmHg)	11 ± 6	13 ± 6	NS

NS = nonsignificant.

of immunosuppression and cellular rejection on the vasculopathy (Mehra et al. 1997). A higher daily dose of cyclosporine was found to be protective from adverse cardiac events (Mehra et al. 1997). Therefore, our data are concordant with the concept that heterogeneity of myocardial perfusion represents small vessel alteration in heart transplant recipients rather than false-positive findings (Puskas et al. 1997).

Abnormal IBS patterns vs. heterogeneity of perfusion and pathologic changes

In this study, patients or myocardial segments could be classified into normal or abnormal IBS patterns by analyzing the parameters of amplitude, phase, and phase-compensated amplitude. These abnormal IBS patterns were associated significantly with pathologic changes (cardiomyocyte hypertrophy and/or interstitial fibrin deposition) and ²⁰¹thallium perfusion defects. Therefore, there is an alteration of acoustic impedance that is caused by variation in tissue elastic modulus and is influenced by abnormal perfusion and pathologic changes. And, this

alteration of acoustic impedance during sarcomere shortening results in the time-varying changes in backscattered energy represented by amplitude and phase-compensated amplitude. Our data are compatible with the previous reports (O'Brien et al. 1995; Wickline et al. 1985). In addition, the peak-dose heart rate was significantly higher in patients with abnormal pathologic findings (150 ± 12 vs. 136 ± 23 beats/min) and also in patients with abnormal IBS patterns (151 ± 12 vs. 140 ± 19 beats/min). Therefore, there are still functional changes of myocardium in these heart recipients despite patent coronary angiography and minimal acute myocardial rejection.

Cardiomyocyte hypertrophy and interstitial fibrin deposition

There is one report describing the prevention of cardiac hypertrophy in mice by cyclosporine through calcineurin inhibition (Sussman et al. 1998). In this study, there was no significant difference of cyclosporine levels in patients with or without cardiomyocyte hyper-

trophy. Our findings are compatible with the results reported by Rowan and Billingham (1990). Therefore, the pathogenesis of cardiomyocyte hypertrophy in transplanted hearts may be calcineurin-independent. On the other hand, no clinical parameters were associated with the cardiomyocyte hypertrophy except white blood cell count. The significance of this finding is unclear. Interstitial fibrin deposition in biopsy during the first month after transplantation has been reported to identify patients at high risk for developing coronary artery disease or graft failure (Labarrere et al. 1998). However, there was no association of $^{201}\text{Thallium}$ perfusion defects and interstitial fibrin deposition in the present study. No clinical parameters were associated with the fibrin deposits except recipient age. Therefore, the significance of this finding deserves further study.

Study limitations

Our study has several limitations. First, cyclic variation of IBS is dependent on the angle between fiber orientation and ultrasonic beam, called anisotropy (Wickline et al. 1985). To avoid the phenomenon of anisotropy, we used the antero-septal, midinferior, junction of midposterior and midlateral segments in which the myocardial fibers are kept oriented as perpendicular to the incident US beam as possible. We have analyzed IBS of the 40 patent coronary vessel territories in our previous study (Lin et al. 1998a). The difference of phase in these regions (region 1, 2 and 3) was insignificant ($p = 0.346$). On the other hand, IBS data are influenced by image quality. The heart transplant recipients are often obese and their echo-windows are limited. However, the body mass index was similar between patients of group A and group B in the present study. Second, using visual analysis rather than quantitative analysis to detect perfusion defect may reduce the sensitivity of $^{201}\text{Thallium}$ imaging. Third, we did not use intracoronary ultrasonography to evaluate the lumen diameters and intimal changes of coronary arteries. Therefore, the seeming normal coronary angiography may underestimate the prevalence of transplant coronary vasculopathy. Finally, the biopsies were taken from the right side of the interventricular septum. The biopsy of right heart may underestimate the true prevalence of left ventricular pathology. However, taking biopsy from left ventricle is not routinely applicable for heart transplant recipients. There was also lack of pathology of healthy age-matched subjects. Because the prevalence of histologic abnormalities was high in heart transplant recipients, the specificity of IBS could not be exactly deduced without such control group.

SUMMARY

Abnormal IBS patterns are associated significantly with perfusion heterogeneity and pathologic changes in heart transplant recipients without evident acute myocardial rejection. There is no association between abnormal IBS patterns and dobutamine-induced dyssynergy in these patients. IBS provides a noninvasive approach for detection of myocardial changes in transplanted hearts without evident acute rejection.

Acknowledgements—This study was supported in part by grant NSC 89-2314-B-002-432 from the National Science Council, Taipei, Taiwan.

REFERENCES

- Angermann CE, Nassan K, Stempfle HU, et al. Recognition of acute cardiac allograft rejection from serial integrated backscatter analyses in human orthotopic heart transplant recipients: Comparison with conventional echocardiography. *Circulation* 1997;95:140–150.
- Armstrong AT, Binkley PF, Baker PB, Myerowitz PD, Leier CV. Quantitative investigation of cardiomyocyte hypertrophy and myocardial fibrosis over 6 years after cardiac transplantation. *J Am Coll Cardiol* 1998;32:704–710.
- Arnese M, Fioretti PM, Cornel JM, et al. Akinesia becoming dyskinesia during high dose dobutamine stress echocardiography: a marker of myocardial ischemia or a mechanical phenomenon? *Am J Cardiol* 1994;73:896–899.
- Castaldo M, Funaro S, Veneroso G, Agati L. Detection of residual tissue viability within the infarct zone in patients with acute myocardial infarction: Ultrasonic integrated backscatter analysis versus dobutamine stress echocardiography. *J Am Soc Echocardiogr* 2000;13:358–367.
- Devereux RB, Reichek N. Echocardiographic determination of left ventricular mass index in man: Anatomical validation of the method. *Circulation* 1977;55:613–618.
- Finch-Johnston AE, Gussak HM, Mobley J, et al. Dependence of "apparent" magnitude on the time-delay of cyclic variation of myocardial backscatter. *Ultrasound Med Biol* 1999;25:759–762.
- Finch-Johnston AE, Gussak HM, Mobley J, et al. Cyclic variation of integrated backscatter: Dependence of time delay on the echocardiographic view used and the myocardial segment analyzed. *J Am Soc Echocardiogr* 2000;3:9–17.
- Ho FM, Huang PJ, Liau CS, et al. Dobutamine stress echocardiography compared with dipyridamole thallium-201 single-photon emission computed tomography in detecting coronary artery disease. *Eur Heart J* 1995;16:570–575.
- Ho YL, Lin LC, Yen RF, et al. Significance of dobutamine-induced ST-segment elevation and T wave pseudonormalization in patients with Q-wave myocardial infarction: Simultaneous evaluation by dobutamine stress echocardiography and $^{201}\text{Thallium}$ SPECT. *Am J Cardiol* 1999;84:125–129.
- Ho YL, Wu CC, Huang PJ, et al. Assessment of coronary artery disease in women by dobutamine stress echocardiography: Comparison with thallium-201 single-photon emission computed tomography and exercise electrocardiography. *Am Heart J* 1998;135:655–662.
- Hsu RB, Chu SH, Wang SS, et al. Low incidence of transplant coronary artery disease in Chinese heart recipients. *J Am Coll Cardiol* 1999;33:1573–1577.
- Huang PJ, Yen RF, Chieng PU, Chen ML, Su CT. Do β -blockers affect the diagnostic sensitivity of dobutamine stress thallium-201 single photon emission computed tomographic imaging? *J Nucl Cardiol* 1998;5:34–39.
- Iskandrian AS, Heo J, Askenase A, Segal BL, Helfant RH. Thallium imaging with single photon emission computed tomography. *Am Heart J* 1987;114:852–865.
- Johnson DE, Alderman EL, Schroeder JS, et al. Transplant coronary

artery disease: Histologic correlations with angiographic morphology. *J Am Coll Cardiol* 1991;17:449-457.

Koskinen PK, Lemstrom KB, Hayry PJ. How cyclosporine modified histological and molecular events in the vascular wall during chronic rejection of rat cardiac allografts. *Am J Pathol* 1995;146:972-980.

Labarrere CA, Nelson DR, Faulk WP. Myocardial fibrin deposits in the first month after transplantation predict subsequent coronary artery disease and graft failure in cardiac allograft recipients. *Am J Med* 1998;105:207-213.

Levy D, Savage DD, Garrison RJ, et al. Echocardiographic criteria of left ventricular hypertrophy: The Framingham Heart Study. *Am J Cardiol* 1987;59:956-960.

Lin LC, Wu CC, Ho YL, et al. Ultrasonic tissue characterization for coronary care unit patients with acute myocardial infarction. *Ultrasound Med Biol* 1998;24:187-196.

Lin LC, Wu CC, Ho YL, et al. Ultrasonic tissue characterization in predicting residual ischemia and myocardial viability for patients with acute myocardial infarction. *Ultrasound Med Biol* 1998;24:1107-1120.

Masuyama T, Valentine HA, Gibbons R, Schnittger I, Popp RL. Serial measurement of integrated ultrasonic backscatter in human cardiac allografts for the recognition of acute rejection. *Circulation* 1990;81:829-839.

Mehra MR, Ventura HO, Chambers RB, et al. The prognostic impact of immunosuppression and cellular rejection on cardiac allograft vasculopathy: Time for a reappraisal. *J Heart Lung Transplant* 1997;16:743-751.

O'Brien PD, O'Brien WD, Rhyne TL, Warltier DC, Sagar KB. Relation of ultrasonic backscatter and acoustic propagation properties to myofibrillar length and myocardial thickness. *Circulation* 1995;91:171-175.

Pickering JG, Boughner DR. Fibrosis in the transplanted heart and relation to donor ischemic time. *Circulation* 1990;81:949-958.

Puskas C, Kosch M, Kerber S, et al. Progressive heterogeneity of myocardial perfusion in heart transplant recipients detected by thallium-201 myocardial SPECT. *J Nucl Med* 1997;38:760-765.

Rowan RA, Billingham ME. Pathological changes in the long-term transplanted heart: A morphometric study of myocardial hypertrophy, vascularity, and fibrosis. *Hum Pathol* 1990;21:767-772.

Schiller NB, Shah PM, Crawford M, et al. for the Am Society of Echocardiography Committee on standards, subcommittee on quantitation of two-dimensional echocardiograms. Recommendations for quantitation of the left ventricle by two-dimensional echocardiography. *J Am Soc Echocardiogr* 1989;2:358-367.

Schoen FJ. The heart. In: Cotran RS, Kumar V, Collins T, eds. Robbin's pathologic basis of disease. 6th edition. Philadelphia: Saunders; 1999:583.

Schulman DS, Herman BA, Edwards TA, Ziady G, Uretsky BF. Diastolic dysfunction in cardiac transplant recipients: An important role in the response to increased afterload. *Am Heart J* 1993;112:435-442.

Senior R, Sridhara BS, Anagnostou E, et al. Synergistic value of simultaneous stress dobutamine sestamibi single-photon-emission computed tomography and echocardiography in the detection of coronary artery disease. *Am Heart J* 1994;128:713-718.

Spes CH, Klauss V, Mudra H, et al. Diagnostic and prognostic value of serial dobutamine stress echocardiography for noninvasive assessment of cardiac allograft vasculopathy. *Circulation* 1999;100:509-515.

St Goar FG, Fausto JP, Aderman EL, et al. Intracoronary ultrasound in cardiac transplant recipients: In vivo evidence of "angiographic silent" intimal thickening. *Circulation* 1992;85:979-987.

Sussman MA, Lim HW, Gude N, et al. Prevention of cardiac hypertrophy in mice by calcineurin inhibition. *Science* 1998;281:1690-1693.

Takiuchi S, Ito H, Iwakura K, et al. Ultrasonic tissue characterization predicts myocardial viability in early stage of reperfused acute myocardial infarction. *Circulation* 1998;97:356-362.

Unverferth DV, Baker PB, Swift SE, et al. Extent of myocardial fibrosis and cellular hypertrophy in dilated cardiomyopathy. *Am J Cardiol* 1986;57:816-820.

Valentine HA, Appleton CP, Hatle LK, et al. A hemodynamic and Doppler echocardiographic study of ventricular function in long-term cardiac allograft recipients. *Circulation* 1989;79:66-75.

Weis M, von Scheidt W. Cardiac allograft vasculopathy. *Circulation* 1997;96:2069-2077.

Wickline SA, Thomas LJ III, Miller JG, Sobel BE, Perez JE. A relationship between ultrasonic integrated backscatter and myocardial contractile function. *J Clin Invest* 1985;76:2151-2159.

Wickline SA, Thomas LJ, Miller JG, Sobel BE, Perez JE. Sensitive detection of the effects of reperfusion on myocardium by ultrasonic tissue characterization with integrated backscatter. *Circulation* 1986;74:389-400.

Winters GL, Schoen FJ. Graft arteriosclerosis-induced myocardial pathology in heart transplant recipients: Predictive value of endomyocardial biopsy. *J Heart Lung Transplant* 1997;16:985-993.

Yeung AC, Davis SF, Hauptmann PJ, et al. Incidence of progression of transplant coronary artery disease over 1 year: Results of a multicenter trial with use of intravascular ultrasound. *J Heart Lung Transplant* 1995;14:S215-S220.